Polarized absorption and energy levels of $LiNbO_3$:Tm and $LiNbO_3$(MgO):Tm

1993 J. Phys.: Condens. Matter 5 5301

(http://iopscience.iop.org/0953-8984/5/30/010)

J. Phys.: Condens. Matter 5 (1993) 5301–5312. Printed in the UK

Polarized absorption and energy levels of $LiNbO_3$:Tm and $LiNbO_3$(MgO):Tm

L Núñez and F Cussó

Departamento Física de Materiales, C-IV, Universidad Autónoma de Madrid, 28049 Madrid, Spain

Received 22 March 1993

Abstract. The polarized absorption spectra of Tm^{3+} ions in $LiNbO_3$ and $LiNbO_3$(MgO) crystals, at 20 K, are presented. The Stark levels of the different multiplets up to 28 000 cm^{-1} are identified. The results are consistent with C_3 symmetry for the rare-earth ions and a singlet (A) character for the lower Stark level of the ground state. Several transitions show additional structure, which indicates multi-site occupancy for the Tm^{3+} ions. The effect of MgO codoping, which includes the appearance of new absorption bands, is also discussed.

1. Introduction

Monolithic integration of active electro-optic devices within a laser material has boosted interest in the optical properties of rare-earth-doped lithium niobate.

In the late 1960s, laser oscillation was obtained in crystals doped with Nd, Ho and Tm [1], and recently the combination with existing technologies of planar waveguide production has proved that it is possible to construct low-threshold integrated devices [2, 3].

The inhibition of photorefractive damage in $LiNbO_3$ doped with approximately 5% MgO further increased interest in this material, which has been used either in miniature bulk lasers or in waveguiding structures [2–5].

Some recent spectroscopic investigations, using site selection techniques [6–9], have indicated that details such as the different sites that the ions can occupy in the $LiNbO_3$ lattice, and the role played by the stabilizing Mg ions and their interactions with the active ions, are needed in order to understand fully the optical performance of these materials.

Most work has focused on a few ions, mainly Nd^{3+}, although other ions are obviously of interest. Tm^{3+} ions offer a number of characteristics which make them interesting, including a suitable absotption for $Al_xGa_{1-x}As$ diode pumping as well as several laser-active IR transitions [10].

Unfortunately, the level structure of Tm^{3+} ions is such that the visible and near-infrared transitions involve levels having a high multiplicity which make the identification of the different multiplets difficult [11–13]. A full level characterization, which is needed in order to attempt any detailed site-selective study, is still lacking.

In the present work the low-temperature (20 K) polarized absorption spectra of Tm^{3+} ions in $LiNbO_3$ and $LiNbO_3$(MgO) crystals, which allows identification of the different transitions involved, is presented.

0953-8984/93/305301+12$07.50

2. Experimental procedure

$LiNbO_3$:Tm^{3+} and $LiNbO_3$(MgO):Tm^{3+} crystals were grown in our laboratory by the Czochralski technique in Pt crucibles from a lithium niobate melt of grade I Johnson–Mathey powder. Thulium oxide and magnesium oxide were used as dopants.

The thulium concentrations, as measured by the Rutherford back-scattering technique, were 1.7×10^{20} cm^{-3} and 8.3×10^{19} cm^{-3} for the singly (Tm) and doubly (Tm–Mg) doped crystals, respectively. MgO was added in a 6% Mg–Nb molar fraction in the melt.

Samples were cut with their faces parallel or perpendicular to the *c*-axis (optic axis) of the crystals. The orientation of this axis was previously confirmed by x-ray diffraction measurements.

Polarized absorption spectra, between 350 and 2500 nm, were recorded with a Cary 17 spectrophotometer using a Glan–Thompson calcite polarizer.

Low-temperature (20 K) absorption measurements were taken using a close-cycle He cryostat.

The emission spectrum of $LiNbO_3$:Tm^{3+} in the range 785–845 nm was measured at liquid-helium temperature (LHT) using a flux-helium cryostat. Excitation was achieved using a CW Ti–sapphire laser (SP 3900); the emission was dispersed by a monochromator of 25 cm focal length and detected with a Si photodiode.

3. Experimental results

Trivalent rare-earth ions enter the $LiNbO_3$ lattice, substituting on either (or simultaneously) Li^+ or Nb^{5+} sites, both having C_3 site symmetry [14]. According to this symmetry [11, 12], each level will split into a number of A and E Stark levels depending on the J-value (table 1).

Table 1. Number of crystal-field states for C_3 symmetry.

	Number of states	
J	A	E
2	1	2
3	3	2
4	3	3
5	3	4
6	5	4

It is well known that for Tm^{3+} ions the visible and near-infrared transitions are of an electric dipole nature. Only the transition from the fundamental $^3H_6$ to the excited $^3H_5$ level has a non-negligible magnetic dipole contribution [15].

The polarization characters of the electric dipole transitions between A and E levels as established by group theory considerations are summarized in table 2, where π and σ stand for light with the electric field parallel and perpendicular, respectively, to the *c* axis of the crystal with the light propagating perpendicular to this axis and α stands for light propagating parallel to the *c* axis.

It can be seen that, in this symmetry, polarization spectroscopy provides, in principle, a good selection between the different transitions, provided that the ground-state character would be well established.

Table 2. Electric-dipole selection rules for C_3 symmetry.

	A	E
A	π	σ, α
E	σ, α	π, σ, α

In order to determine precisely the Stark components of the $^3H_6$ ground level, the (unpolarized) emission spectrum $^3F_4 \rightarrow {}^3H_6$ of $LiNbO_3$:Tm^{3+} at LHT after Ti–sapphire laser excitation has been obtained.

The structure of the ground-state level $^3H_6$ is clearly resolved, showing nine components, in accordance with the expected multiplicity for this level in C_3 symmetry. The energies of the different Stark levels are given in table 3. The observed structure is in good agreement with the partial structure already identified from the $^3H_4 \rightarrow {}^3H_6$ emission in the range 1.6–1.8 μm [13].

Table 3. Stark structure of the ground state ($^3H_6$) of the Tm^{3+} ions in $LiNbO_3$ at liquid-helium temperature, obtained from the $^3F_4 \rightarrow {}^3H_6$ emission.

Stark level	λ (nm)	ΔE (cm^{-1})
Z_1	792.9	0
Z_2	795.5	41
Z_3	798.9	94
Z_4	803.8	171
Z_5	812.2	298
Z_6	817.7	382
Z_7	822.4	452
Z_8	828.0	533
Z_9	833.1	608

It is important to note that the fundamental and the first excited Stark levels are well separated, showing an energy difference ($\Delta E \simeq 40$ cm^{-1}) large enough to ensure negligible population of the excited level at a low temperature (20 K).

This guarantees that the observed absorption bands at the low temperature involve transitions from a single Stark level (Z_1) to the different excited-state components, simplifying the application of the selection rules. In fact, as will be shown throughout this work, the absorption bands (light propagating perpendicular to the c axis) have a well defined polarization character (σ or π). This indicates, according to the selection rules given in table 2, that the transitions always involve a singlet (A) level, which is therefore the character to be associated with the lower Stark level of the ground state.

Once this assignment has been done, it is possible to proceed to identify the components of the excited-state levels from the low-temperature polarized absorption measurements.

The highest-energy absorption band of Tm^{3+} ions detectable for $LiNbO_3$ is the $^3H_6 \rightarrow {}^1D_2$ transition shown in figure 1. Although this transition is superimposed on the absorption edge of $LiNbO_3$, it is possible to identify the structure arising from the different Stark levels.

The $^1D_2$ level has the lowest degeneracy ($J = 2$) of the observed bands (together with the $^3F_2$ level) and therefore the symmetry assignment is easier than for the remaining transitions.

According to the C_3 symmetry selection rules, two σ- and one π-polarized lines are expected. This is experimentally confirmed, as can be seen in figure 1 where two main

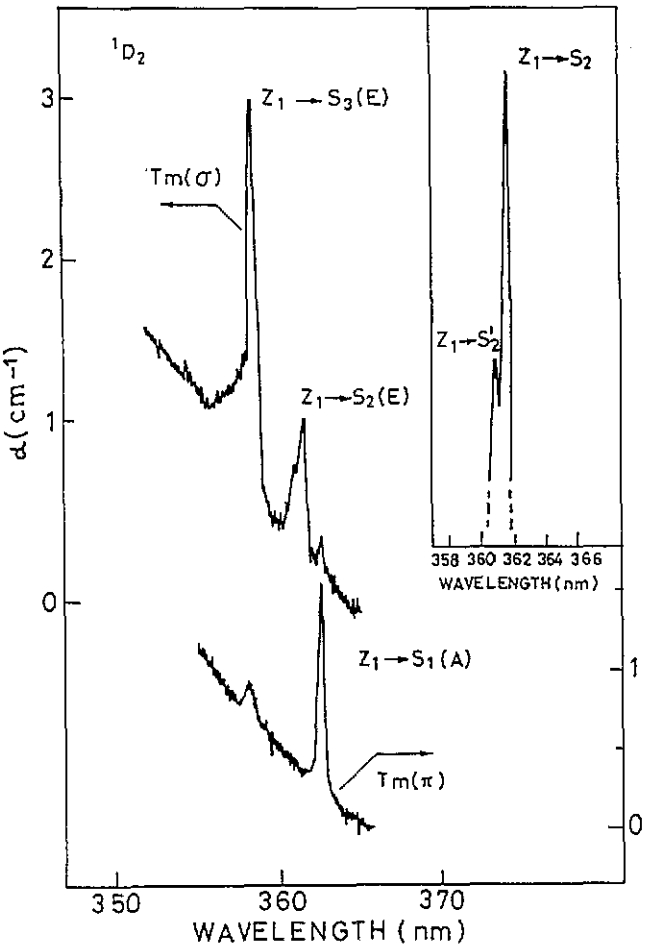

Figure 1. Polarized absorption spectra for the $^3H_6 \rightarrow {}^1D_2$ transition of Tm^{3+} ions in $LiNbO_3$. A detail of the $Z_1 \rightarrow S_2(E)$ peak is shown in the inset.

bands in the σ spectrum and a single band in the π spectrum appear. The positions of these lines and the associated Stark levels are listed in table 4.

Minor contributions to the σ and π spectra at wavelengths coincident with the dominant peaks in the opposite polarization can be attributed to a partial depolarization produced by the experimental set-up or to some slight misorientation of the sample.

In spite of the simplicity of this particular level, additional features have already appeared. The transition to the second Stark level ($Z_1 \rightarrow S_2$) shows a doublet structure which has been expanded in the inset in figure 1. The appearance of this doublet for a single Stark level is an indication of the existence of two different sites for the Tm^{3+} ions in the $LiNbO_3$ lattice, as has been observed for other ions [6–9]. We shall indicate with a prime the additional lines which, belonging to a given Stark level, could correspond to different lattice sites.

In the crystals codoped with 6% MgO, the $^3H_6 \rightarrow {}^1D_2$ transition exhibits a very similar structure to that of the singly doped crystals, except for some broadening of the bands, so that the same level assignment is applicable.

Table 4. Observed energy levels and polarization characters of Tm^{3+} ions in $LiNbO_3$. The asterisk indicates lines appearig only for Mg-codoped crystals.

$^{2S+1}L_J$	λ (nm)	E (cm^{-1})	Transition	Polarization
$^3H_4$	1792.4	5579.0	$Z_1 \rightarrow Y_\alpha(A)^*$	π
	1764.8	5666.2	$Z_1 \rightarrow Y_1(A)$	π
	1761.2	5678.0	$Z_1 \rightarrow Y_1'(A)$	π
	1756.7	5692.4	$Z_1 \rightarrow Y_2(E)$	σ, α
	1755.1	5697.8	$Z_1 \rightarrow Y_2'(E)$	σ, α
	1745.6	5728.6	$Z_1 \rightarrow Y_2''(E)$	σ, α
	1696.5	5894.6	$Z_1 \rightarrow Y_3(E)$	σ, α
	1664.3	6008.4	$Z_1 \rightarrow Y_4(A)$	π
	1660.6	6022.1	$Z_1 \rightarrow Y_5(E)$	σ, α
	1654.6	6043.6	$Z_1 \rightarrow Y_5^1(E)$	σ, α
	1645.7	6076.6	$Z_1 \rightarrow Y_6$ (A)	π
	1614.6	6193.6	$Z_1 \rightarrow Y_\beta(A)^*$	π
$^3H_5$	1216.1	8223.0	$Z_1 \rightarrow X_1(E)$	σ, π, α
	1208.5	8274.4	$Z_1 \rightarrow X_\alpha'(E)^*$	σ, π, α
	1191.7	8391.7	$Z_1 \rightarrow X_2(E)$	σ, α
	1189.6	8406.2	$Z_1 \rightarrow X_3(E)$	σ, α
	1179.4	8479.1	$Z_1 \rightarrow X_4(A)$	π
	1176.8	8497.8	$Z_1 \rightarrow X_5(A)$	π
	1168.3	8559.7	$Z_1 \rightarrow X_6(A)$	π
	1158.7	8630.4	$Z_1 \rightarrow X_7(E)$	σ, π, α
	1148.7	8705.8	$Z_1 \rightarrow X_8(E)$	σ, π, α
	1142.2	8755.3	$Z_1 \rightarrow X_9(E)$	σ, π, α
$^3F_4$	793.5	12602.3	$Z_1 \rightarrow W_1(E)$	σ, α
	790.2	12655.7	$Z_1 \rightarrow W_2(A)$	π
	785.0	12739.5	$Z_1 \rightarrow W_3(A)$	π
	779.7	12825.0	$Z_1 \rightarrow W_4(E)$	σ, α
	773.5	12928.8	$Z_1 \rightarrow W_5(E)$	σ, α
	771.0	12969.8	$Z_1 \rightarrow W_6(A)$	π
	765.0	13071.5	$Z_1 \rightarrow W_\alpha(A)^*$	π
$^3F_3$	689.7	14498.5	$Z_1 \rightarrow V_1'(A)$	π
	689.1	14512.2	$Z_1 \rightarrow V_1(A)$	π
	688.9	14515.9	$Z_1 \rightarrow V_2'(E)$	σ, α
	687.6	14543.4	$Z_1 \rightarrow V_2(E)$	σ, α
	685.4	14591.0	$Z_1 \rightarrow V_3'(E)$	σ, α
	684.6	14606.1	$Z_1 \rightarrow V_3(E)$	σ, α
	684.3	14613.7	$Z_1 \rightarrow V_4'(A)$	π
	683.1	14640.2	$Z_1 \rightarrow V_4(A)$	π
	681.6	14671.9	$Z_1 \rightarrow V_5'(A)$	π
	680.2	14701.2	$Z_1 \rightarrow V_5(A)$	π
	679.5	14716.5	$Z_1 \rightarrow V_5''(A)$	π
$^3F_2$	663.2	15079.6	$Z_1 \rightarrow U_1(E)$	σ, α
	662.4	15095.7	$Z_1 \rightarrow U_2(A)$	π
	655.0	15267.2	$Z_1 \rightarrow U_\alpha(A)^*$	π
	651.9	15339.1	$Z_1 \rightarrow U_3(E)$	σ, α
$^1G_4$	479.7	20845.3	$Z_1 \rightarrow T_\alpha(A)^*$	π
	475.5	21029.6	$Z_1 \rightarrow T_1(E)$	σ, α
	475.0	21052.6	$Z_1 \rightarrow T_2(A)$	π
	466.4	21439.7	$Z_1 \rightarrow T_3(E)$	σ, α
	465.3	21496.8	$Z_1 \rightarrow T_3'(E)$	σ, α
	465.0	21507.2	$Z_1 \rightarrow T_4(A)$	π
	464.6	21523.6	$Z_1 \rightarrow T_4^1(A)$	π
	463.7	21565.3	$Z_1 \rightarrow T_5(E)$	σ, α
	463.4	21581.8	$Z_1 \rightarrow T_5'(E)$	σ, α
	462.6	21617.6	$Z_1 \rightarrow T_5''(E)$	σ, α
	460.8	21700.1	$Z_1 \rightarrow T_6(A)$	π
	459.4	21767.1	$Z_1 \rightarrow T_\beta(A)^*$	π
$^1D_2$	362.8	27566.7	$Z_1 \rightarrow S_1(A)$	π
	361.6	27656.8	$Z_1 \rightarrow S_2(E)$	σ, α
	360.9	27711.1	$Z_1 \rightarrow S_2'(E)$	σ, α
	358.3	27912.1	$Z_1 \rightarrow S_3(E)$	σ, α

Following the order of descending energy, the next transition observed for Tm^{3+}-doped $LiNbO_3$ is the $^3H_6 \rightarrow {}^1G_4$ transition. Figures 2(*a*) and (*b*) present the π-polarized absorption spectra of Tm- and Tm–Mg-doped crystals, respectively.

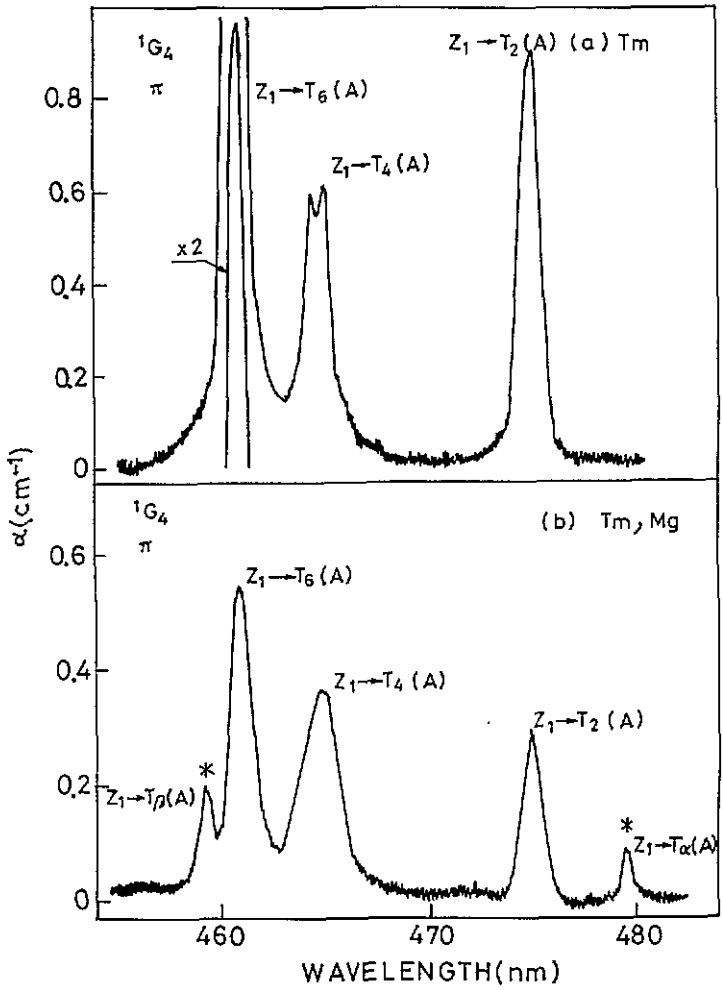

Figure 2. π-polarized absorption spectra for the $^3H_6 \rightarrow {}^1G_4$ transition of (*a*) $LiNbO_3$:Tm^{3+} and (*b*) $LiNbO_3$(MgO):Tm^{3+}.

It can be seen that, in accordance with the assumption of C_3 symmetry for Tm^{3+} ions, three main bands at 475.0, 465.0 and 460.8 nm appear (figure 2(*a*)). As already observed for the $^1D_2$ transition, some additional structure can be detected, as the splitting of the $Z_1 \rightarrow T_4$ transition, suggesting again a multi-site occupancy of Tm^{3+} ions in the $LiNbO_3$ lattice.

The π-polarized spectrum of the Tm–Mg-doped crystals (figure 2(*b*)) deserves special comment. In addition to the main bands T_2(A), T_4(A) and T_6(A), which are coincident with those of the Tm-doped crystal, two new bands T_α(A), and T_β(A) arise on both sides of the spectrum.

The appearance of new bands in Mg-codoped $LiNbO_3$ has already been observed for Nd^{3+} ions by using luminescence techniques [6, 7] and in the infrared emission spectrum of Tm-doped crystals [13]. These bands have been attributed to the appearance of new sites where the impurity (Tm in this case) is affected by the Mg ions.

These new lines, which are induced by the presence of Mg ions in the crystal and which appear also in other transitions (see table 4), will be denoted with an asterisk.

In relation to the main bands already appearing in the crystals without Mg, it can be observed (figure 2(*b*)) that Mg codoping affects the linewidth, producing a general broadening of the spectrum. It can also be observed that the splitting of the $Z_1 \rightarrow T_4$ transition is affected, with a drastic reduction in the intensity of the high-energy component T_4', which is now only revealed in the asymmetry of the band.

C_3 symmetry would also predict three σ-polarized lines for this transition ($^3H_6 \rightarrow {}^1G_4$) which is in fact the structure observed for either $LiNbO_3$:Tm^{3+} or $LiNbO_3$(MgO):Tm^{3+}. Except for some broadening in the latter crystal, the lines are coincidental and their positions are given in table 4.

The next transition ($^3H_6 \rightarrow {}^3F_2$) can also be explained with C_3 symmetry selection rules. Although these absorption bands are the weakest of the optical spectrum, in accordance with the values of the matrix elements associated with this transition [15], the two expected σ-polarized and one expected π-polarized absorption bands are detected for the Tm-doped crystal (table 4). A weak new π-polarized band is also added in the Tm–Mg-doped crystal (table 4).

The clearest example of the existence of splitting in the absorption bands, confirming the occurrence of several Tm sites as well as evidence that Mg-codoping affects these occupancies, is provided by the next ($^3H_6 \rightarrow {}^3F_3$) transition.

The corresponding π-polarized absorption spectrum of Tm-doped $LiNbO_3$ is shown in figure 3 (upper curve). From the selection rules, three π-polarized lines are expected, while the observed spectrum shows six lines grouped in three doublets whose components have similar intensities and small energy differences.

The fact that the two components have the same polarization character (π) and comparable intensities indicates that Tm^{3+} ions occupy, in similar numbers, two 'optical sites' with the same symmetry. Although the experimental data could also be explained assuming different numbers of ions for each site compensated because of different oscillator strengths to give the same absorbance, this possibility seems unrealistic.

Let us also indicate that we have used the term 'optical site' to indicate that the sites detected using optical techniques do not necessarily have to be coincident with 'lattice sites' strictly speaking. Although the possibility that Tm^{3+} ions enter the crystal in both Li^+ and Nb^{5+} sites looks highly plausible (this possibility will be further discussed later), this cannot be unambiguously ascertained by optical techniques alone.

The lower curve in figure 3 shows the absorption of Mg-codoped samples. Although the broadening of the bands tends to obscure some of the structure, it can still be observed, as with the $^3H_6 \rightarrow {}^1G_4$ transition, that the relative intensities of the doublet components change with the presence of Mg in the crystals. In particular, the low-energy (V_1') components are strongly reduced.

This is consistent with the luminescence experiments reported for Nd^{3+}-doped $LiNbO_3$(MgO) where similar effects have been found [6].

Let us also indicate that, in spite of the narrow structures detectable in this transition, no additional Mg-induced bands have been detected, at variance with other multiplets.

The σ spectrum associated with the $^3H_6 \rightarrow {}^3F_3$ transition (not shown) is of much weaker intensity and presents again the two expected σ components according to C_3 symmetry.

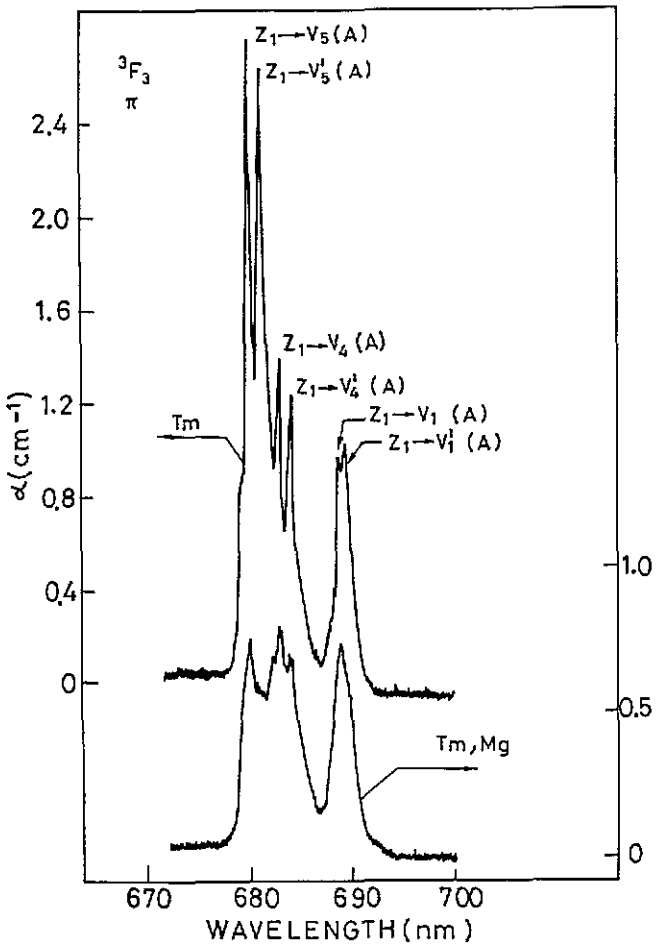

Figure 3. π-polarized absorption spectra for the $^3H_6 \rightarrow {}^3F_3$ transition of $LiNbO_3:Tm^{3+}$ (upper curve) and $LiNbO_3(MgO):Tm^{3+}$ (lower curve), showing three main components with a clear doublet structure.

Their positions are given in table 4.

The next transition in descending energy corresponds to the $^3H_6 \rightarrow {}^3F_4$ absorption band which covers the 750–800 nm spectral range. This range is especially relevant in relation to $Al_xGa_{1-x}As$ diode laser pumping of Tm^{3+} ions [10].

The main absorption band arises at around 794 nm with a σ character (99%). Weaker additional bands, two σ and three π polarized, appear in accordance with C_3 symmetry (table 4).

For the doubly doped crystal, the spectra are very similar to those of the singly doped crystal, except for some broadening of the bands. A weak new line at 765 nm in the π-polarized spectrum is the only new feature associated with Mg codoping.

All the transitions which have already been presented were forced electric dipole in nature and magnetic dipole forbidden. The next absorption spectrum (figure 4), associated with the $^3H_6 \rightarrow {}^3H_5$ transition, is the only spectrum having a sizable magnetic dipole contribution.

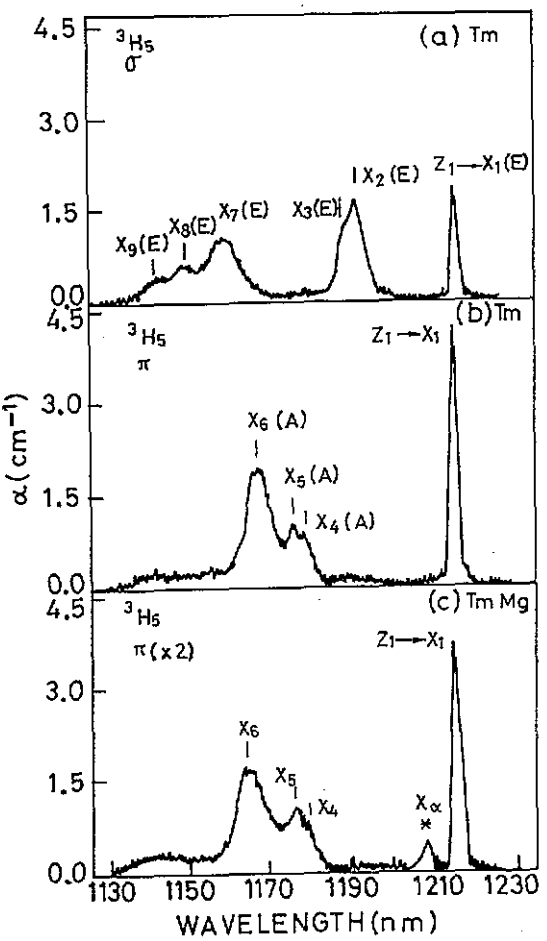

Figure 4. Polarized absorption spectra for the $^3H_6 \rightarrow {}^3H_5$ transition of (*a*), (*b*) $LiNbO_3:Tm^{3+}$ and (*c*) $LiNbO_3(MgO):Tm^{3+}$.

The magnetic character is clearly observed for the absorption line at 1215 nm ($Z_1 \rightarrow X_1$) which can be detected for σ, π and α polarizations. This fact can be used to label this line as arising from an A→E transition. This seems to be the case also for the bands, partially overlapped, which appear in the region 1140–1160 nm. The remaining lines have a well defined σ or π character, with the α polarization spectra coincident with the σ polarization spectra, so that no magnetic dipole contribution affects these components.

According to table 1, seven sublevels are expected, whereas the observed structure in our experimental results exceeds that number. Although this again indicates that Tm^{3+} ions can be found in different sites, in this case the observed bands cannot be unambiguously assigned or grouped into a number of doublets, as previously in the case of the $^3H_6 \rightarrow {}^3F_3$ transition. Therefore, the levels associated with the different bands experimentally observed have been simply labelled from X_1 to X_9, in increasing order of energy. Their positions and polarization character are detailed in table 4.

Magnesium ions produce a general broadening, as described for the previous transitions. A new absorption band, which appears in the π, σ and α spectra, is observed at 1208.5 nm

(figure 4(*c*)).

Finally, the lowest-energy absorption band is associated with the $^3H_6 \rightarrow {}^3H_4$ transition, where from group theory arguments (tables 1 and 2), three σ- and three π-polarized absorption bands are expected.

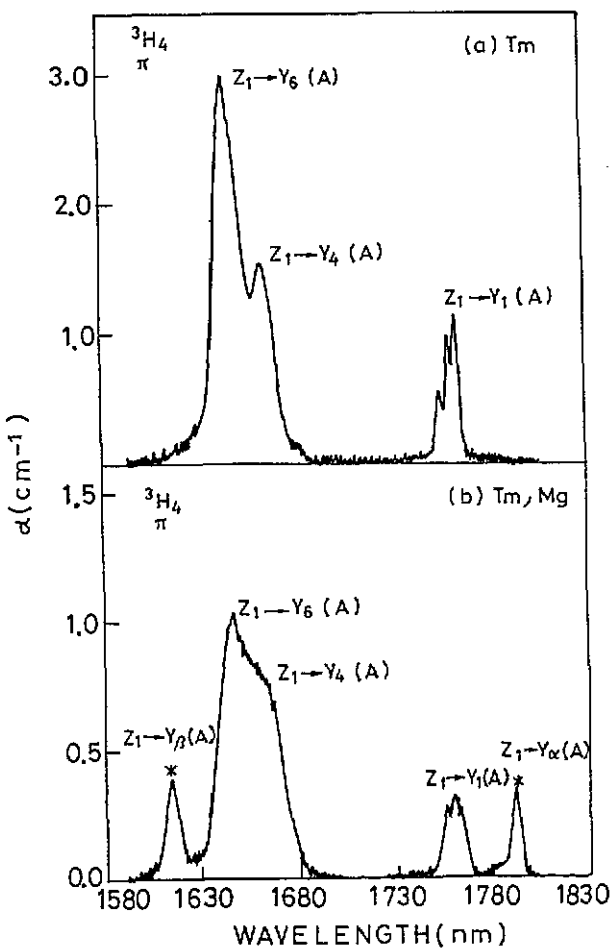

Figure 5. π-polarized absorption spectra for the $^3H_6 \rightarrow {}^3H_4$ transition of (*a*) $LiNbO_3:Tm^{3+}$ and (*b*) $LiNbO_3(MgO):Tm^{3+}$.

The π-polarized spectrum, which is shown in figure 5, resembles that of the $^3H_6 \rightarrow {}^1G_4$ transition presented in figure 2. Three main bands appear in the $LiNbO_3:Tm^{3+}$ crystal, with some of the bands showing additional structure. In this case (figure 5(*a*)) the splitting of the lowest-energy component into a doublet becomes particularly clear. The third smaller peak is coincident with a dominant peak in σ polarization (table 4) and it can be attributed to partial depolarization or misorientation of the crystal.

Mg codoping causes the broadening of the bands and changes the relative intensities of the split components, as was already observed for the 680 nm transition ($^3H_6 \rightarrow {}^3F_3$). Additionally, the appearance of new Mg-induced bands, on both sides of the spectrum, is particularly apparent.

In the σ spectrum (not shown), three main bands are detected, for both $LiNbO_3$ and $LiNbO_3$(MgO) crystals. Additional structures are also detected, which are particularly evident in the lower-energy component. The positions of the bands are summarized in table 4.

4. Discussion

The polarized absorption spectra of Tm^{3+}-doped $LiNbO_3$ reveal a neatly differentiated polarization character, which can be interpreted considering C_3 symmetry for the rare-earth ions and a singlet (A) character for the lower-energy ground-state Stark level.

Several transitions, including many singlet-to-singlet transitions, have shown the appearance of additional structure, which indicates multi-site occupancy for Tm^{3+} ions. The $^3H_6 \rightarrow {}^3F_3$ transition (figure 3) provides a particularly clear example.

In those bands where splitting is more evident, it has been confirmed that the polarization character (π for an A$\rightarrow$A transition) is conserved, indicating that the site symmetry is also preserved.

The fact that the intensities of the subbands are comparable indicates also that the different 'optical sites' appear in similar numbers.

Li^+, Nb^{5+} and the intrinsic vacancy are the natural sites, having trigonal symmetry, in $LiNbO_3$ crystals. Provided that no metal impurity has been found to occupy the intrinsic vacancy [14], Li^+ and Nb^{5+} sites appear as reasonable candidates for Tm^{3+} location. In that case, the 'optical sites' would strictly correspond to the 'lattice sites'.

An additional piece of information is provided by the changes induced by Mg codoping. Two main facts occur: one is the appearance of new Tm^{3+} bands, and the other is the change induced in the relative heights of the split components.

Similar effects, detected by luminescence techniques, have been reported [6] for Nd^{3+}-doped $LiNbO_3$(MgO). The effect of Mg codoping on the size of the Tm^{3+} absorption bands could be interpreted in the same way. Provided that Mg^{2+} ions are incorporated into the $LiNbO_3$ lattice by entering the Li^+ sites [14], this implies competition with the Tm^{3+} ions which would affect the populations in the different sites.

This could happen either as direct competition with the Tm^{3+} ions also occupying Li^+ sites or indirectly via the removal of the so-called anti-sites (Nb^{5+} in Li^+ sites), which would return to their positions, replacing the Tm^{3+} ions located in Nb^{5+} sites. Therefore the assignment of the components to Tm^{3+} in Li^+ or Nb^{5+} sites cannot be unambiguously decided.

The new Tm^{3+} bands associated with Mg codoping could also be tentatively explained in the same law as for Nd^{3+}-doped crystals, in which these new bands are considered to arise from rare-earth ions occupying Nb^{5+} lattice sites, perturbed by a Mg^{2+} ion placed in a neighbouring Li^+ site [6].

Nevertheless, these assignments are only tentative and, although the optical data are fully consistent with these interpretations, it is clear that they cannot be ascertained using optical methods alone and that other techniques, which could provide direct information on the lattice location of the impurities, are needed.

Recently, ion-beam techniques have confirmed multi-site occupancy for rare-earth ions in $LiNbO_3$ [16]. Unfortunately, only preliminary studies are available for Tm^{3+}-doped crystals [17], which seem to indicate Li^+ location plus a fraction of ions occupying other non-identified lattice sites. In order to confirm this point, further studies combining optical and ion-beam techniques are still needed.

Acknowledgments

This work has been partially supported by Comisión Interministerial de Ciencia y Tecnología under contract MAT92-0250. We wish also to express our gratitude to Professor F Jaque for his critical reading of the manuscript.

References

[1] Johnson L F and Ballman A A 1969 *J. Appl. Phys.* **40** 297
[2] Lallier E, Pocholle J P, Papuchon M, Grezes-Besset C, Pelletier E, DeMicheli M, Li M J, He Q and Ostrowsky D B 1989 *Electron. Lett.* **25** 1491
[3] Field S J, Hanna D C, Shepherd D P, Tropper A C, Chandler P J, Townsend P D and Zhang L 1991 *Opt. Lett.* **16** 481
[4] Bryan D A, Gerson R and Tomaschke H E 1984 *Appl. Phys. Lett.* **44** 847
[5] Fan T Y, Cordova-Plaza A, Digonnet M J F, Byer R L and Shaw H J 1986 *J. Opt. Soc. Am.* B **3** 140
[6] Lifante G, Cussó F, Jaque F, Sanz-García J A, Monteil A, Varrel B, Boulon G and García-Solé J 1991 *Chem. Phys. Lett.* **176** 482
[7] Tocho J O, Camarillo E, Cussó F, Jaque F and García-Solé J 1991 *Solid State Commun.* **80** 575
[8] Camarillo E, García-Solé J, Cussó F, Agulló-López F, Sanz-García J A, Han T P J, Jaque F and Henderson B 1991 *Chem. Phys. Lett.* **185** 505
[9] Tocho J O, Jaque F, García-Solé J, Camarillo E, Cussó F and Muñoz-Santiuste J E 1992 *Appl. Phys. Lett.* **60** 3206
[10] Fan T Y and Byer R L 1988 *IEEE J. Quantum Electron.* **QE-24** 895
[11] Hüfner S 1978 *Optical Spectra of Transparent Rare Earth Compounds* (New York: Academic)
[12] Henderson B and Imbusch G F 1989 *Optical Spectroscopy of Inorganic Solids* ed H Fröhlich, A J Heeger, P B Hirsch, N F Mott and R Brook (Oxford: Clarendon)
[13] Tocho J O, Núñez L, Sanz-García J A, Cussó F, Hanna D C, Tropper A C, Field S J, Shepherd D P and Large A C 1991 *J. Physique IV Coll.* **1** C7 293
[14] Rebouta L, Soares J C, da Silva M F, Sanz-García J A, Dieguez E and Agulló-López F 1990 *Nucl. Instrum. Methods* B **50** 428
[15] Spector N, Reisfeld R and Boehm L 1977 *Chem. Phys. Lett.* **49** 49
[16] Rebouta L, Soares J C, da Silva M F, Sanz-García J A, Dieguez E and Agulló-López F 1992 *J. Mater. Res.* **7** 130
[17] Rebouta L 1992 *PhD Thesis* University of Lisboa